Journal of Alloys and Compounds 506 (2010) 372–376

Contents lists available at ScienceDirect

Journal of Alloys and Compounds

journal homepage: www.elsevier.com/locate/jallcom

# The effects of calcination temperature on the electrochemical performance of $LiMnPO_4$ prepared by ultrasonic spray pyrolysis

Seung-Min Oh [a], Sung Woo Oh [a], Seung-Taek Myung [b], Sung-Man Lee [c], Yang-Kook Sun [a,*]

[a] Department of Energy Engineering, Hanyang University, Seoul 133-791, South Korea
[b] Department of Chemical Engineering, Iwate University, 4-3-5 Ueda, Morioka, Iwate 020-8551, Japan
[c] Department of Advanced Materials Science and Engineering, Kangwon National University, Chunchon, Kangwon 200-701, South Korea

ARTICLE INFO

*Article history:*
Received 10 January 2010
Received in revised form 6 July 2010
Accepted 6 July 2010
Available online 14 July 2010

*Keywords:*
Coating materials
Nano-structured materials
X-ray diffraction
Transmission electron microscopy
Scanning electron microscopy

ABSTRACT

Carbon-coated $LiMnPO_4$ powders were prepared by ultrasonic spray pyrolysis. The effects of calcination temperature on the microstructure and electrochemical performance of C-$LiMnPO_4$ were investigated. X-ray diffraction (XRD) studies showed that the crystallite size varied with calcination temperature. Scanning electron microscopy (SEM) and transmission electron microscopy (TEM) observations revealed that the calcination temperature had a strong influence on the morphology of the prepared final powder, and therefore the subsequent electrochemical performance of the material. The C-$LiMnPO_4$ powders prepared at 650 °C exhibited excellent electrochemical performance with a discharge capacity of 118 mAh $g^{-1}$.


## 1. Introduction

$LiMPO_4$ (M = Fe, Mn, Co and Ni) materials have attracted interest as potential positive electrode materials for rechargeable Li-ion batteries [1]. Among these, $LiFePO_4$ has been a focus of interest because of its low cost, non-toxicity, and outstanding thermal stability [2,3]. However, $LiFePO_4$ has a lower working voltage than other positive electrode materials such as $LiCoO_2$, $LiNiCoO_2$, and $Li_2MnO_4$ because of the $Fe^{2+}/Fe^{3+}$ redox reaction at 3.4 V vs. $Li/Li^+$. Therefore, $LiMnPO_4$ has been proposed as a candidate positive electrode material because its redox potential (4.1 V vs. $Li/Li^+$) is higher than that of $LiFePO_4$ (3.4 V vs. $Li/Li^+$) [1], which indicates that $LiMnPO_4$ has a higher energy density than $LiFePO_4$. Furthermore, $LiMnPO_4$ is compatible with the present electrolytes used for 4 V class positive electrodes such as $LiCoO_2$ and $LiMn_2O_4$ oxide cathode materials. The theoretical energy density of $LiMnPO_4$ (697 Wh $kg^{-1}$) is higher than that of $LiFePO_4$ (586 Wh $kg^{-1}$). Unfortunately, the electronic conductivity of $LiMnPO_4$ (<$10^{-10}$ S/cm) is much lower than that of $LiFePO_4$ ($1.8 \times 10^{-9}$ S/cm) [4,5].

Recently, several research groups have attempted to optimize the electrical conductivity of $LiMnPO_4$ and have demonstrated that the intrinsic low rate capability can be enhanced by nano-sizing the particles; furthermore, carbon coating of $LiMnPO_4$ has been shown to significantly improve the electronic conductivity between particles. For example, C-$LiMnPO_4$ with a reversible capacity of 112 mAh $g^{-1}$ at C/20 was obtained by a combination of spray pyrolysis synthesis using $N_2/H_2$ (97/3 vol%) gas and wet ball milling with acetylene black as a carbon source [6]. A platelet-like material with a capacity of 80 mAh $g^{-1}$ at C/20 was obtained by a precursor based solid-state reaction [7]. Xiao et al. also prepared a phase-pure $MnPO_4 \cdot H_2O$ by thermal lithiation with LiAc and ketjenblack as carbon sources: the resulting material showed a discharge capacity of 115 mAh $g^{-1}$ at the C/20 rate [8].

Although the above results exhibited improved electrochemical performance by nano-sizing particles and carbon coating, we speculate that carbon coating with calcination temperature should be optimized to further improve the electrochemical properties of $LiMnPO_4$. For this reason, we investigate the carbon conversion effect of C-$LiMnPO_4$ materials varying calcination temperatures.

In this study, we report on the synthesis of $LiMnPO_4$ cathode materials via an ultrasonic spray pyrolysis method. Sucrose was employed as a carbon coating source. In attempt to optimize carbon coating on $LiMnPO_4$, the calcination temperatures varied under $Ar/H_2$ (96/4 vol%) atmosphere for carbon conversion. Herein, we investigate the effects of calcination temperature on the structural and electrochemical properties of the $LiMnPO_4$. Details of synthetic process and the corresponding electrochemistry of carbon-coated $LiMnPO_4$ are introduced.

* Corresponding author. Tel.: +82 2 2220 0524; fax: +82 2 2282 7329.
*E-mail address:* yksun@hanyang.ac.kr (Y.-K. Sun).

0925-8388/$ – see front matter © 2010 Elsevier B.V. All rights reserved.
doi:10.1016/j.jallcom.2010.07.010

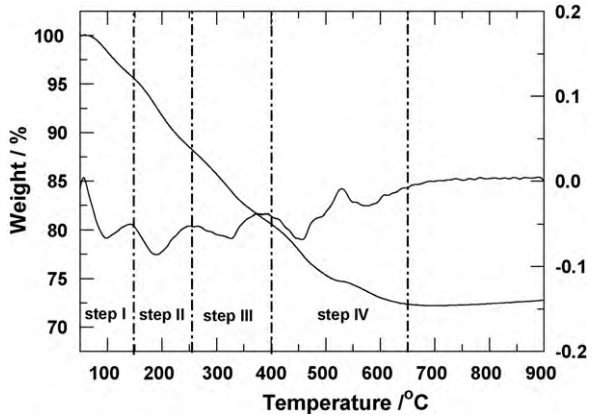


**Fig. 1.** (a) Thermo-gravimetric analysis (TGA) of $LiMnPO_4$ synthetic powder.

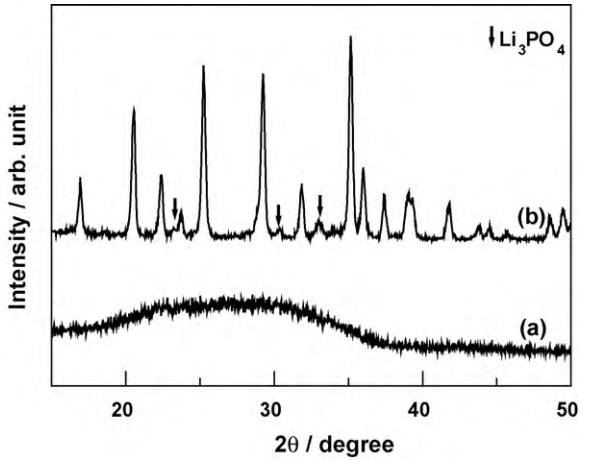


**Fig. 2.** XRD patterns of (a) as-received powders and (b) $LiMnPO_4$ powder after a 500 °C heat treatment.

## 2. Experimental

$LiMnPO_4$ powders were prepared by an ultrasonic spray pyrolysis method. Stoichiometric amounts of manganese nitrate tetrahydrate ($Mn(NO_3)_2{\cdot}4H_2O$, Junsei) and lithium dihydrogen-phosphate ($LiH_2PO_4$, Aldrich) were dissolved in distilled water at a molar ratio of Li:Mn of 1:1. The dissolved solution was added to a citric acid and sucrose aqueous solution (molar ratio of $LiMnPO_4$:citric acid:sucrose = 1:0.2:0.05). Citric acid was used as a chelating agent in the synthesis of a homogeneous mixed solution ($Mn(NO_3)_2{\cdot}4H_2O$, $LiH_2PO_4$, and sucrose) while sucrose was used to prevent the crystallite growth of $LiMnPO_4$ particles [9]. The starting solution was atomized using an ultrasonic nebulizer with a resonant frequency of 1.7 MHz. The resulting aerosol stream was introduced into a vertical quartz reactor heated to 400 °C. The inner diameter and length of the quartz reactor were 50 and 1200 mm, respectively. The flow rate of the air used as a carrier gas was 10 L $min^{-1}$. As-received powders were then heat-treated at 500 °C for 10 h in an air atmosphere to obtain anhydrous $LiMnPO_4$ powders (hereafter referred to as 'precursors'). The obtained precursors were mixed with sucrose as a carbon coating source by ball milling at a speed of 100 rpm for 20 h. The mixtures of $LiMnPO_4$ and sucrose were then calcined at 550–700 °C for 10 h in an $Ar/H_2$ (96/4 vol%) mixture, resulting in carbon-coated $LiMnPO_4$ (hereafter C-$LiMnPO_4$). To determine the specific surface area of the prepared C-$LiMnPO_4$, nitrogen sorption measurements were taken using a Quantachrom Autosorb-1 after samples were degassed for 4 h at 200 °C.

Powder X-ray diffraction (XRD, Rint-2000, Rigaku, Japan) using Cu-Kα radiation over the $2\theta$ range of 15°–50° with a step size of 0.03° was employed to identify the crystalline phase of the synthesized materials. Lattice parameters were calculated by a least squares method. The particle morphologies of the precursors and powders were observed using scanning electron microscopy (SEM, JSM 6400, JEOL) and transmission electron microscopy (TEM, JEOL, 2010). Galvanostatic charge/discharge cycling was performed using a R2032-type coin cell. Electrodes were fabricated using a mixture of active powder (85 wt%), carbon black (7.5 wt%), and polyvinylidene fluoride (PVDF) in *N*-methyl-2-pyrrolidone (7.5 wt%). The slurry was applied on aluminum foil and dried overnight at 110 °C under vacuum. Lithium foil (Cyprus Foote Mineral Co.) was used as the negative electrode. The electrolyte solution used was 1 M $LiPF_6$ in a mixture of ethylene carbonate (EC) and diethyl carbonate (DEC) in a 1:1 volume ratio (Ukseung Industries Inc., Korea). The cells were cycled in a constant current-constant voltage mode at a C/20 rate (8.5 mA $g^{-1}$) to 4.5 V, held at 4.5 V until the C/100 rate, and then discharged to 2.7 V at a C/20 rate (1 C = 170 mA $g^{-1}$).

## 3. Results and discussion

The thermal-gravimetric analysis (TGA) curve obtained from the as-synthesized powder is shown in Fig. 1. The total weight loss was about 28%, and weight loss did not occur at temperatures over 650 °C. Four discrete weight loss regions were observed at 30–150, 150–250, 250–400, and 400–650 °C, respectively. The weight loss in the temperature range of 30–150 °C was attributed to the removal of adsorbed water. The second step of weight loss between 150 and 250 °C was attributed to the decomposition of nitrate ions and the dehydration of sucrose [10,11]. The weight loss in the temperature range of 250–400 °C was attributed to the decomposition of sucrose and citric acid [12], while the fourth weight loss in the temperature range of 400–650 °C was attributed to the removal of remaining organics trapped inside the pores [11]. Further heating at higher temperatures only improved the crystallinity of the samples.

The XRD patterns of the as-synthesized sample and the as-synthesized sample heated at 500 °C in air are shown in Fig. 2. The X-ray diffraction pattern of the as-synthesized sample shows an amorphous phase (Fig. 2a). Teng et al. [13] reported a similar phenomenon for $LiFe_{0.9}Mg_{0.1}PO_4$. After heating the precursor at 500 °C in air, the amorphous phase of the as-synthesized sample transformed into a crystalline phase. All the reflection peaks (Fig. 2b) could be indexed as orthorhombic $LiMnPO_4$ with lattice parameters of $a$ = 10.4499 Å, $b$ = 6.1052 Å, $c$ = 4.7386 Å, which are in agreement with the reported values (JCPDS card no. 74-0375). Furthermore, an impurity was observed at $2\theta$ = 23.2, 30.3, and 33°; this was indexed as $Li_3PO_4$ caused by insufficient calcination.

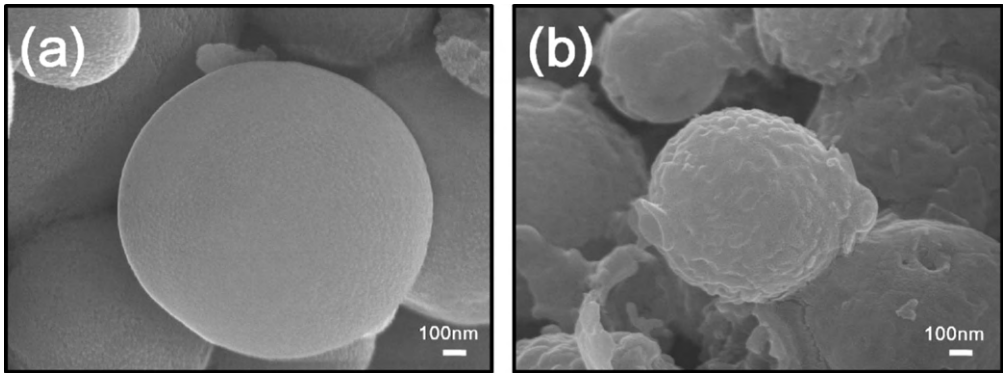


**Fig. 3.** SEM images of (a) as-received powders and (b) $LiMnPO_4$ after heat treatment at 500 °C.

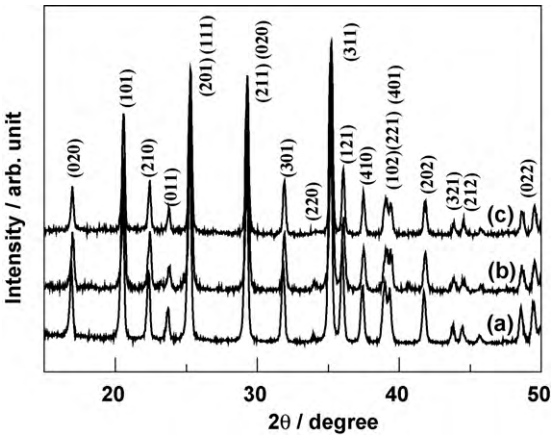


**Fig. 4.** XRD patterns of C-$LiMnPO_4$ powders calcined at (a) 550 °C, (b) 650 °C, and (c) 700 °C.

**Table 1**
Amount of carbon in C-$LiMnPO_4$ samples synthesized at various calcination temperatures.

| Calcination temperature (°C) | Carbon content (wt%) |
|---|---|
| 550 | 3.305 |
| 650 | 3.083 |
| 700 | 2.907 |

Scanning electron micrographs (SEM) of the as-received sample and $LiMnPO_4$ heated at 500 °C are shown in Fig. 3. The as-synthesized sample consisted of particles with a spherical morphology with an average particle size of 2–3 μm, as shown in Fig. 3a. The $LiMnPO_4$ particles retained a spherical morphology after heating at 500 °C, as shown in Fig. 3b, even though the particle size decreased slightly due to the evaporation of volatile compounds such as nitrates and organics. However, some broken particles were also observed and the $LiMnPO_4$ particles had a walnut shape.

The X-ray diffraction patterns of C-$LiMnPO_4$ produced at various calcination temperatures from the precursor ($LiMnPO_4$) and sucrose mixtures are shown in Fig. 4. All samples could be indexed to the orthorhombic *Pnma* space group (JCDPS card no. 74-0375) based on a well-ordered olivine structure. Sucrose provided a carbon source for homogeneous coating of the $LiMnPO_4$ particles to improve the electronic conductivity of the final product. No diffraction peaks were derived from crystalline carbon (graphite) [14]; therefore, it is likely that the carbon in the composite was amorphous. According to elemental analysis (C, H, N, S), we found that the carbon content in the products ranged from about 2.9 to 3.3 wt%, as shown in Table 1. The decrease in the carbon content with increasing calcination temperature can be ascribed to the consumption of carbon in a strong reducing atmosphere. Variations in the lattice parameters and unit cell volumes of the prepared powders calcined at various temperatures are shown in Table 2. The lattice parameter was calculated by a least squares method from the XRD patterns shown in Fig. 4. The calculated lattice parameters and cell volume decreased slightly with calcination temperature. Arnold et al. [15] reported a shrinkage of the crystal structure within the crystallographic *a*–*c* plane as synthesis temperature increased.

**Table 2**
Variation in lattice parameters of C-$LiMnPO_4$ prepared at various calcinations temperatures.

| Temperature (°C) | *a* (Å) | *b* (Å) | *c* (Å) | Cell volume (Å$^3$) |
|---|---|---|---|---|
| 550 | 10.4477 | 6.1096 | 4.7455 | 302.906 |
| 650 | 10.4298 | 6.1000 | 4.7324 | 301.084 |
| 700 | 10.4272 | 6.0966 | 4.7317 | 300.798 |

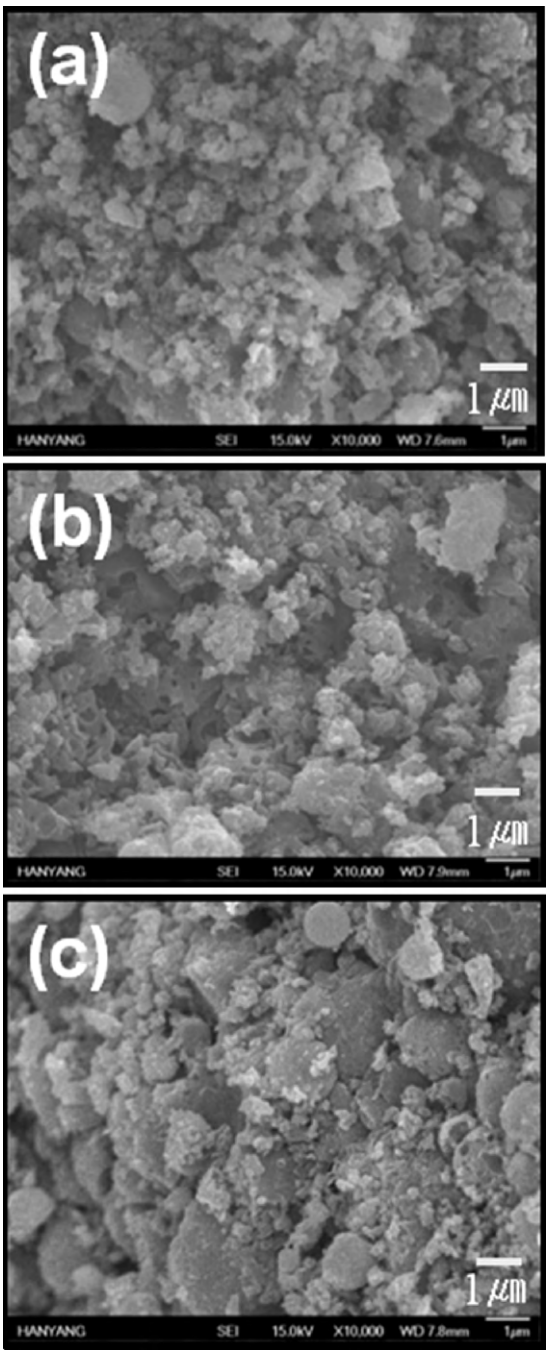


**Fig. 5.** SEM images of C-$LiMnPO_4$ powders calcined at (a) 550 °C, (b) 650 °C, and (c) 700 °C.

We also investigated the effects of calcination temperature on crystallite growth. Crystallite sizes of the prepared C-$LiMnPO_4$ powders were calculated from the major diffraction peaks of $LiMnPO_4$ using Scherrer's equation (Eq. (1)):

$$D_c = \frac{K^*\lambda}{\theta_{1/2}\cos\theta_B} \quad (1)$$

where $K^*$ is a constant (*ca.* 0.9), λ is the X-ray wavelength (1.5418 Å), $\theta_B$ is the Bragg angle, and $\theta_{1/2}$ is the pure diffraction broadening of a peak at half-height, that is, the full-width at half-maximum depends only on the crystallite dimension. Table 3 shows the variation in XRD crystal size ($D_c$) of the C-$LiMnPO_4$ particles prepared at different calcination temperatures. The crystalline size of the

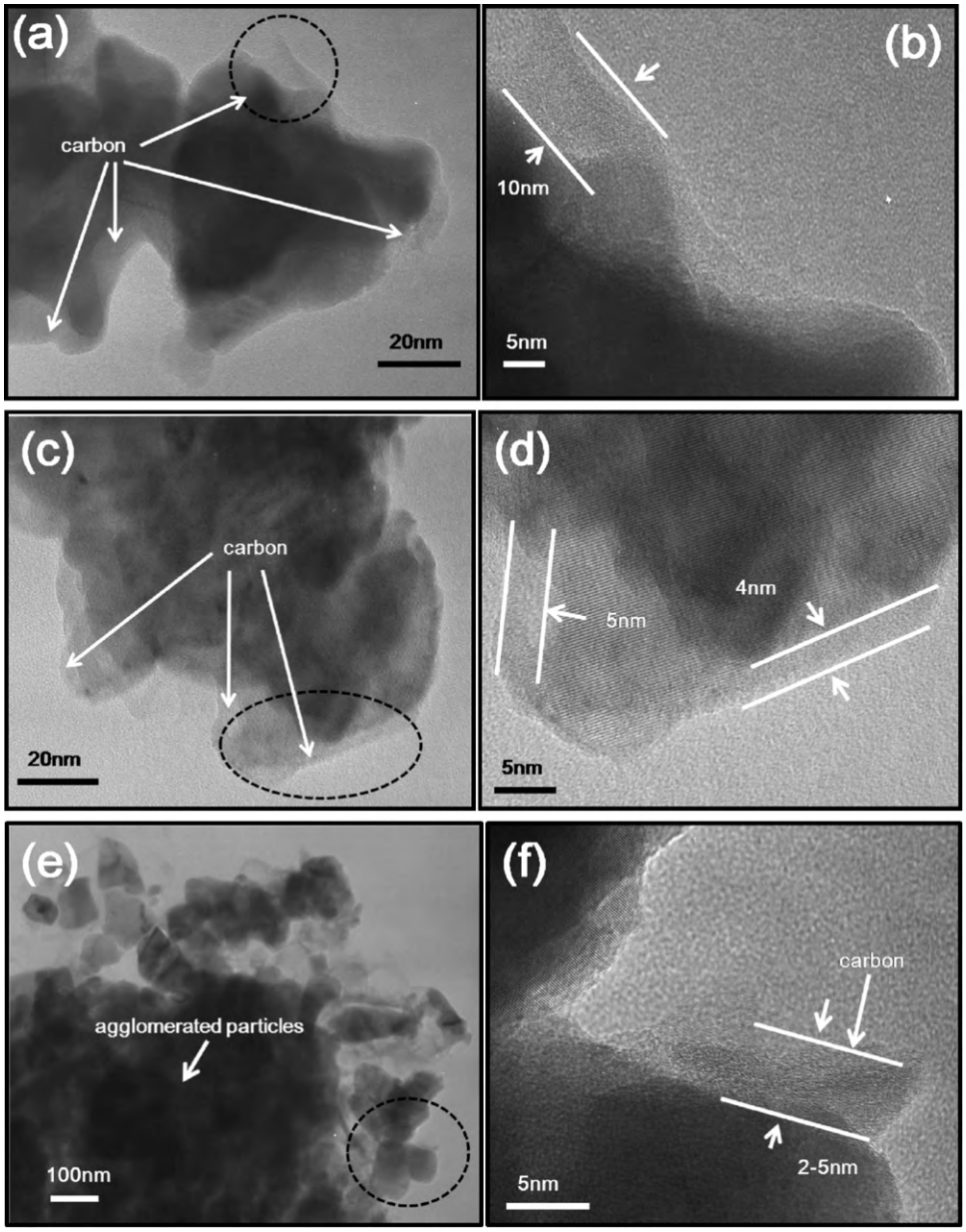


**Fig. 6.** TEM images of C-$LiMnPO_4$ powders calcined at 550 °C (a) low magnification, (b) high magnification; 650 °C (c) low magnification, (d) high magnification; and 700 °C (e) low magnification, (f) high magnification.

**Table 3**
Crystallite and surface area of C-LiMnPO4 powders prepared at various calcination temperatures.

| Temperature (°C) | Crystallite size (nm) | Surface area ($m^2\ g^{-1}$) |
|---|---|---|
| As-received sample | – | 11.80 |
| 550 | 52 | 69.45 |
| 650 | 56 | 66.17 |
| 700 | 60 | 59.90 |

C-$LiMnPO_4$ particles increased according to calcination temperature (from 52 nm at 550 °C to 60 nm at 700 °C). The larger grain size was caused by the growth of crystals, which, in turn, resulted in a decrease in the surface area (Table 3). Note that the specific surface area (11.80 $m^2\ g^{-1}$) of the as-received sample was much smaller than those (69.5 $m^2\ g^{-1}$ at 550 °C, 66.2 $m^2\ g^{-1}$ at 650 °C, and 59.9 $m^2\ g^{-1}$ at 700 °C) of the calcined C-$LiMnPO_4$ powders, indicating that the as-received sample did not completely decompose due to insufficient calcination conditions (low temperatures and a short heating time).

SEM images of the C-$LiMnPO_4$ powders prepared at different temperatures were used to evaluate the effects of calcination temperature on the morphology of the prepared materials. The C-$LiMnPO_4$ powders consisted of particles with a non-spherical shape and small size irrespective of the calcination temperature, as shown in Fig. 5. As temperature increased, a significant increase in particle size and a smoother particle surface were observed. Among the samples, the particle size of the sample calcined at 650 °C showed better uniformity, as shown in Fig. 5b. When the sample was calcined at 700 °C, irregular particles with a smooth surface appeared, and somewhat large agglomerates were observed, probably due to the higher calcination temperature.

To observe the carbon coating layer on the surface of C-$LiMnPO_4$ particles in detail, the C-$LiMnPO_4$ particles were examined by HRTEM. TEM images of the various C-$LiMnPO_4$ particles are shown

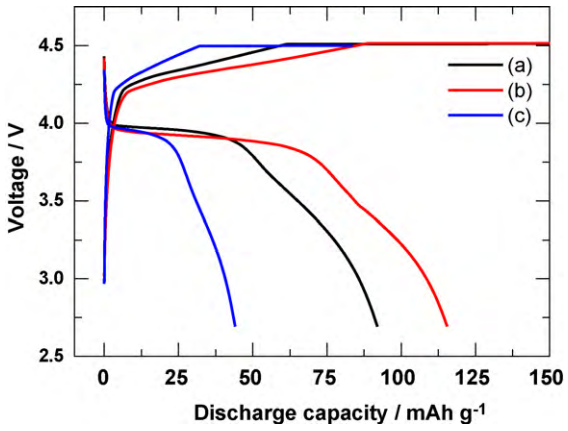


**Fig. 7.** Charge–discharge profiles of Li/C-$LiMnPO_4$ cells cycled between 2.7 and 4.5 V at C/20 (where 1 C = 170 mA $g^{-1}$): $LiMnPO_4$ calcined at (a) 550 °C, (b) 650 °C, and (c) 700 °C.

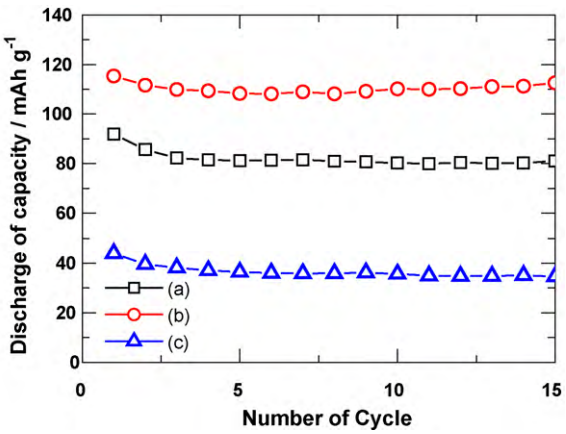


**Fig. 8.** Discharge capacity vs. cycle number of Li/C-$LiMnPO_4$ cells at 25 °C for $LiMnPO_4$ calcined at (a) 550 °C, (b) 650 °C, and (c) 700 °C.

in Fig. 6; the dark regions represent $LiMnPO_4$ particles and the light gray regions correspond to carbon. As shown in the TEM images, the carbon thickness of the three C-$LiMnPO_4$ samples calcined at 550, 650, and 700 °C was estimated to be approximately 10, 4–5, and 2–5 nm, respectively, indicating that the carbon coating layer became thinner as calcination temperature increased. Furthermore, the carbon layer homogeneously coated the particle surface as well as the grain boundaries in the C-$LiMnPO_4$ samples calcined at 550 and 650 °C. In the samples calcined at 550 and 650 °C, the nano-sized primary particles were well dispersed and formed agglomerates with a size of 50–100 nm even though the primary particle size increased slightly at the higher calcination temperature of 650 °C. In contrast, the C-$LiMnPO_4$ powder calcined at 700 °C has a different morphology consisting of highly agglomerated primary particles, which would be expected to decrease electronic conductivity due to a long $Li^+$ ion diffusion path. The C-$LiMnPO_4$ particles calcined at 700 °C also exhibited an irregular coating layer, as shown in Fig. 6f.

The first charge–discharge capacities of Li/C-$LiMnPO_4$ cells prepared at different calcination temperatures are compared in Fig. 7. All the electrodes exhibited electrochemical activity with charge and discharge plateaus around 4.1 V vs. $Li/Li^+$. These plateaus correspond to the $Mn^{3+}/Mn^{2+}$ redox couple accompanied by lithium ion extraction and insertion from/into $LiMnPO_4$ [1,16]. The discharge capacity of the C-$LiMnPO_4$ powder prepared at 650 °C was 118 mAh $g^{-1}$, whereas that of the C-$LiMnPO_4$ powder calcined at 550 and 700 °C was 90 and 44 mAh $g^{-1}$, respectively. The sample prepared at 550 °C had a much lower discharge capacity than that of the sample prepared at 650 °C. The presence of undecomposed organic compounds, which was confirmed by thermo-gravimetric analysis (TGA), the insufficient crystallinity of $LiMnPO_4$, and the insufficient carbonization of sucrose at 550 °C all contributed to the lower discharge capacity despite the small particle size. The discharge capacity of the sample prepared at 700 °C was even worse than that of the sample calcined at 550 °C; the discharge capacity was only 44 mAh $g^{-1}$ at the same C-rate. The dramatic decrease in the capacity of this sample was probably due to the agglomerated primary particles and the heterogeneous carbon coating layer, as shown in Figs. 5c, 6e and f.

Fig. 8 shows the discharge capacities vs. cycle number for the Li/C-$LiMnPO_4$ cells. The C-$LiMnPO_4$ electrode prepared at 650 °C exhibited the highest discharge capacity and a more stable cycle life than the other two samples. The capacity retention of the C-$LiMnPO_4$ electrode prepared at 650 °C was about 97.3% of its initial capacity after 15 cycles, whereas the capacity retention of the C-$LiMnPO_4$ electrodes calcined at 550 and 700 °C was 92.5 and 78.5%, respectively.

## 4. Conclusions

Nano-sized C-$LiMnPO_4$ powders were successfully prepared by ultrasonic spray pyrolysis followed by calcination of the precursor $LiMnPO_4$ and sucrose. Both the microstructure and the electrochemical performance of the C-$LiMnPO_4$ samples were strongly dependent on the calcination temperature. A significant increase in particle size and an irregular carbon coating layer were observed as calcination temperature increased. The C-$LiMnPO_4$ sample prepared at 650 °C exhibited the best electrochemical performance with a discharge capacity of 118 mAh $g^{-1}$ at 1/20 C and a capacity retention of 97.3%.

## Acknowledgements

This work was supported by the National Research Foundation of Korea Grant funded by the Korean Government (MEST) (NRF-2009-C1AAA001-0093307).

## References

[1] A.K. Padhi, K.S. Nanjundaswamy, J.B. Goodenough, J. Electrochem. Soc. 144 (1997) 1188.
[2] S.-Y. Chung, J.T. Bloking, Y.-T. Chiang, Nat. Mater. 1 (2002) 123.
[3] P. Subramanya Herle, B. Ellis, N. Coombs, L.F. Nazar, Nat. Mater. 3 (2004) 147.
[4] M. Yonemura, A. Yamada, Y. Takei, N. Sonoyama, R. Kanno, J. Electrochem. Soc. 151 (2004) A1352.
[5] A. Yamada, Y. Kudo, K.Y. Liu, J. Electrochem. Soc. 148 (2001) A1153.
[6] Z. Bakenov, Taniguchi, Electrochem. Commun. 12 (2010) 75.
[7] N.N. Bramnik, H. Ehrenberg, J. Alloys Compd. 464 (1–2) (2008) 259–264.
[8] J. Xiao, W. Xu, D. Choi, J.-G. Zhang, J. Electrochem. Soc. 157 (2010) A142.
[9] Y. Wang, Y. Wang, E. Hosono, K. Wang, H. Zhou, Angew. Chem. Int. Ed. 47 (2008) 7461.
[10] S.W. Oh, S.H. Park, Y.K. Sun, J. Power Sources 161 (2006) 1314.
[11] C.P. Sibu, S. Rajesh Kumar, P. Mukundan, K.G.K. Warrier, Chem. Mater. 14 (2002) 2876.
[12] Y. Jiugao, W. Ning, Ma. Xiaofei, Starch 57 (2005) 494.
[13] T.-H. Teng, M.-R. Yang, S.-H. Wu, Y.-P. Chiang, Solid-State Commun. 142 (2007) 389.
[14] S.S. Zhang, J.L. Allen, K. Xu, T.R. Jow, J. Power Sources 147 (2005) 234.
[15] G. Arnold, J. Garche, R. Hemmer, S. Ströbele, C. Vogler, M. Wohlfahrt-Mehrens, J. Power Sources 119–121 (2003) 247.
[16] G. Li, H. Azuma, M. Tohda, Electrochem. Solid-State Lett. 5 (2002) 135.